

Supporting Information

d'Errico et al. 10.1073/pnas.0903532106

SI Text

Methodology. Identification of *Nassarius gibbosulus* and *Nassarius circumcinctus* was based on known morphological differences, and size and morphological variability of these species along the Tunisian and the Israeli coast (1–5). *N. gibbosulus* has a broad last whorl, one or two dorsal humps (of which one is massive), and a sharply pointed apex. *N. circumcinctus* features a slender last whorl, no dorsal hump or just a single one (often weakly developed), and a decollated and blunt apex covered by the upper part of the parietal shield. Penultimate and previous whorls show interrupted brown spiral lines in *N. gibbosulus*, and red-brown axial flames in *N. circumcinctus*. The color demarcation of the parietal shield is pale orange in *N. gibbosulus*, and dark brown in *N. circumcinctus*. The archaeological specimens from Taforalt, Rhafas, and Contrebandiers were compared with modern, fossil and archaeological collections of *N. gibbosulus* (Linnaeus 1758) and *N. circumcinctus* (Adams 1852). The modern collections include 158 living and 285 dead *N. gibbosulus* from Djerba Island, Tunisia, collected by two of us (F.d., M.V.) in 2005 (5), and 312 specimens from the Tel Aviv University, dredged in the Haifa Bay, Israel between 1981 and 1983 by H. Hornung (Tel Aviv University Mollusc Collection 34621, 34624, 34625) and E. Gilat (Tel Aviv University Mollusc Collection 34629). It also includes 59 *N. circumcinctus* from Nahariyya, Israel (Tel Aviv University Mollusc Collection 34689), 15 from Yafo, Israel (Tel Aviv University Mollusc Collection 40582), and 33 from the Haifa Bay (Tel Aviv University Mollusc Collection 34676). The natural Pleistocene age collections include four *N. gibbosulus* and three *N. circumcinctus* from the Strombid layer of a Tyrrenian beach close to Monastir, Tunisia (collection Clanzing & Lozouet 1983, Département de Malacologie, Musée National d'Histoire Naturelle, Paris, PL 16160), and more than 30 mostly fractured *Nassarius* sp. collected in 2008 at the base of the Dar-es-Soltan sequence, Rabat, Morocco. The Monastir beach is dated to 126 ± 7 ka (6, 7). Identified by Ruhlmann (8) as layer << M >>, the Dar-es-Soltan stratigraphic unit from which the shells have been recovered has been dated recently by

optically stimulated luminescence (OSL) to ca. 144 ± 9.1 ka and 139.4 ± 6.8 ka (9). The comparative collection from archaeological sites includes two *N. gibbosulus* from Skhul and one from Oued Djebdana (5).

We recorded age class (juvenile, subadult, adult), maximum shell height, and width on all measurable modern, fossil, and archaeological shells. The thickness of the parietal shield on both lateral sides of the shell was measured on 110 *N. gibbosulus* from Djerba biocoenosis, 100 from Djerba thanatocoenosis, and fossil and archaeological specimens. Perforation types and breakage patterns on the dorsal and ventral side of the shells were recorded on the Djerba thanatocoenosis and the archaeological specimens. The maximum and minimum diameter of unbroken perforations was also recorded on the archaeological specimens. All measurements were taken with a digital caliper with the exception of those on the Ifri n'Ammar specimen, recorded on a high quality digital image. When necessary for the analysis, archaeological specimens were cleaned under the microscope with a wet wooden toothpick and a soft brush. The six sides of each shell were digitized at a resolution of 1200 dpi with an Epson Perfection 4990 Photo scanner. Resulting images served as a base from which to produce drawings of the four longitudinal aspects of each shell with Adobe Illustrator. All shells were examined under a Leica Z6 APO microscope equipped with a Coolpix 995 digital camera. Presence of shell fragments and beach gravel stuck in the shells, surface modifications on the shell and perforation edges (perforations made by predators, damage inflicted by bioeroders, marine encrustations, use wear, tool marks, changes of shade and cracks due to heating, postdepositional damage), and pigment residues were photographed and marked on the drawings. The Ifri n'Ammar specimens were identified and analyzed based on photos only.

A comprehensive database of personal ornaments found at Iburomaurusian, Capsian, and Neolithic sites from Morocco, Algeria, and Tunisia has been created by surveying the relevant archaeological literature (10–14). This database includes 210 sites and 72 bead-types.

1. Poppe GT, Goto Y (1991) *European Seashells. Volume I, Polyplacophora, Caudofoveata, Solenogaster, Gastropoda* (Verlag Christa Hemmen, Wiesbaden, Germany).
2. Abbott RT, Dance SP (2000) *Compendium of Seashells* (Odyssey Publishing, El Cajon).
3. Barash A, Danin Z (1992) *Annotated List of Mediterranean Molluscs of Israel and Sinai. Fauna Palaestina – Mollusca I* (The Israel Academy of Sciences and Humanities, Jerusalem).
4. Giannuzzi-Savelli R, Pusateri F, Palmeri A, Ebrey C (2003) *Atlas of the Mediterranean Seashells. Vol. 4, first part, Neogastropoda: Muricoidea* (Edizioni Evolver, Rome).
5. Vanhaeren M, et al. (2006) Middle Paleolithic shell beads in Israel and Algeria. *Science* 312:1785–1788.
6. Hearty PJ, Miller GH, Steams CE, Szabo BJ (1986) Aminostratigraphy of Quaternary shorelines in the Mediterranean basin. *Geol Soc Am Bull* 97:850–858.
7. McLaren SJ, Rowe PJ (1996) The reliability of Uranium-series mollusc dates from the western Mediterranean basin. *Quat Sci Rev* 15:709–717.
8. Ruhlmann A (1951) *The Prehistoric Cave of Dar-es-Soltan* (Collection Hésperis 11, Institut des Hautes Études Marocaines, Larose, Paris) (in French).
9. Barton RNE, Bouzouggar A, Colclutt SN, Schwenninger J-L, Clark-Balzan L, OSL dating of the Aterian levels at Dar es-Soltan I (Rabat, Morocco) and possible implications for the dispersal of modern *Homo sapiens*. *Quat Sci Rev* 28:1914–1931.
10. Camps-Faber H (1960) Prehistoric personal ornaments from North Africa. *Libyca Anthropologie, Préhistoire, Etnographie* VIII:9–220 (in French).
11. Collina-Girard J, Cremades M, Lavaure N (1997) Microscopic analysis of an engraved Iburomaurusian pendant from Ain Aghbal Shelter, Eastern Morocco. *Antiquités Africaines* 33:9–18 (in French).
12. Lubell D (2001) in *Encyclopedia of Prehistory, Vol. 1: Africa*, eds Peregrine PN, Ember M (Kluwer Academic/Plenum Publishers, New York), pp 129–149.
13. Rahmani N (2004) Technological and cultural change among the last hunter-gatherers of the Maghreb: The Capsian (10,000–6000 B.P.). *J World Prehistory* 18:57–105.
14. Roubet C (2006) Subsistence and symbolic behavior of Neolithic shepherds from the eastern Atlasic Maghreb. *C R Acad Sci* 344:441–451.

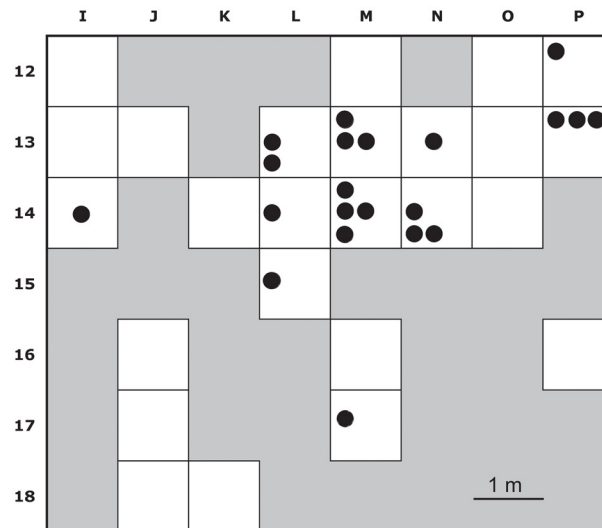
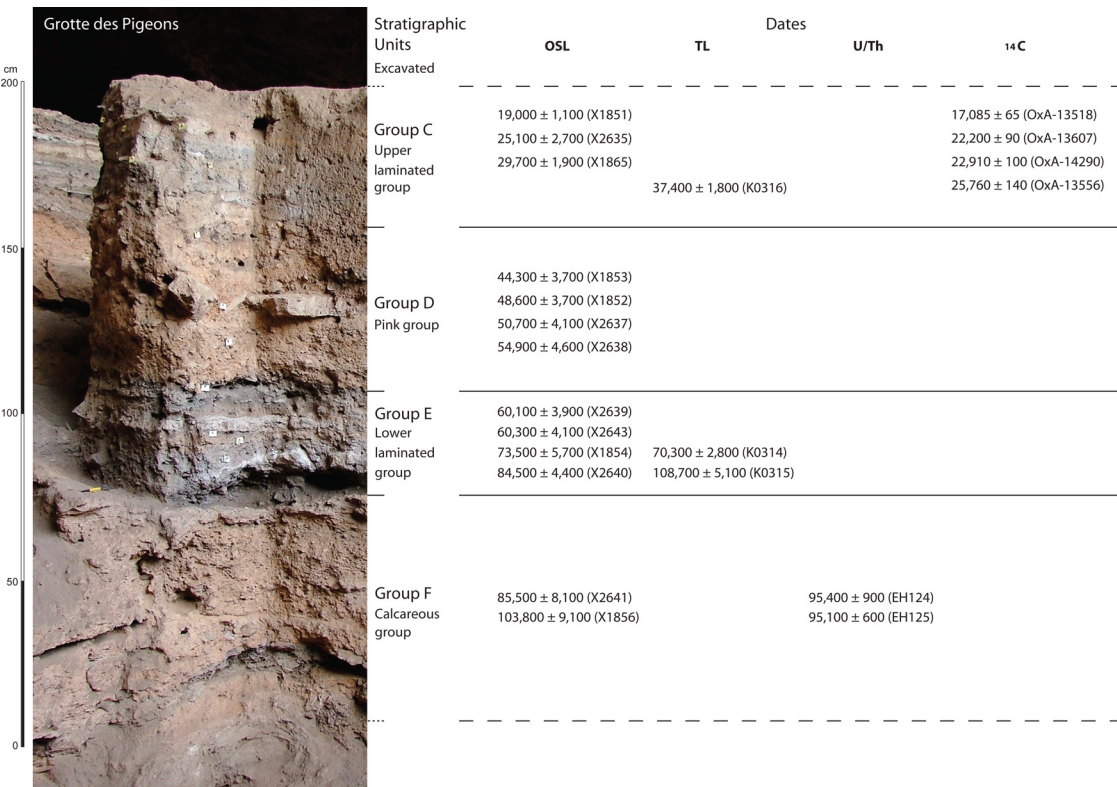


Fig. S1. (Top) Grotte des Pigeons (Taforalt) section with the limits of the main stratigraphic units and the dates for Groups C–F. (Bottom) Spatial distribution of *Nassarius* shells from Group E recovered in situ. Excavated squares are indicated in white.

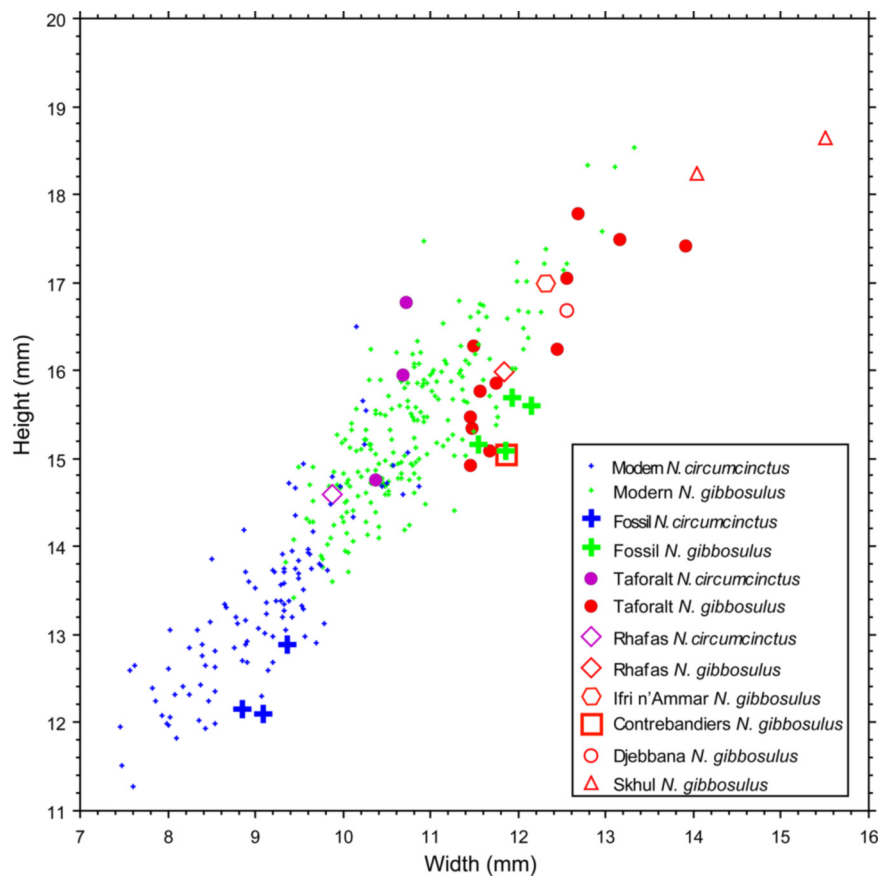


Fig. S2. Scattergram of shell width against shell height of *Nassarius* from modern, fossil and archaeological collections.



Fig. S3. *Nassarius gibbosulus* from Grotte des Pigeons (a and b, n° 5668; c and d, n° 7122) and Rhafas (e and f, n° 145) with a perforation made by a gastropod predator (a) and gravel stuck inside the body whorl (b), elongated pits left by bioeroders on the inner surface of the aperture (c and d) and the parietal wall (e and f). Notice in c–f the presence of red pigment filling the pits. (Scale bars: a = 1 cm; b, c, e, and f = 1 mm; d = 200 μ m.)

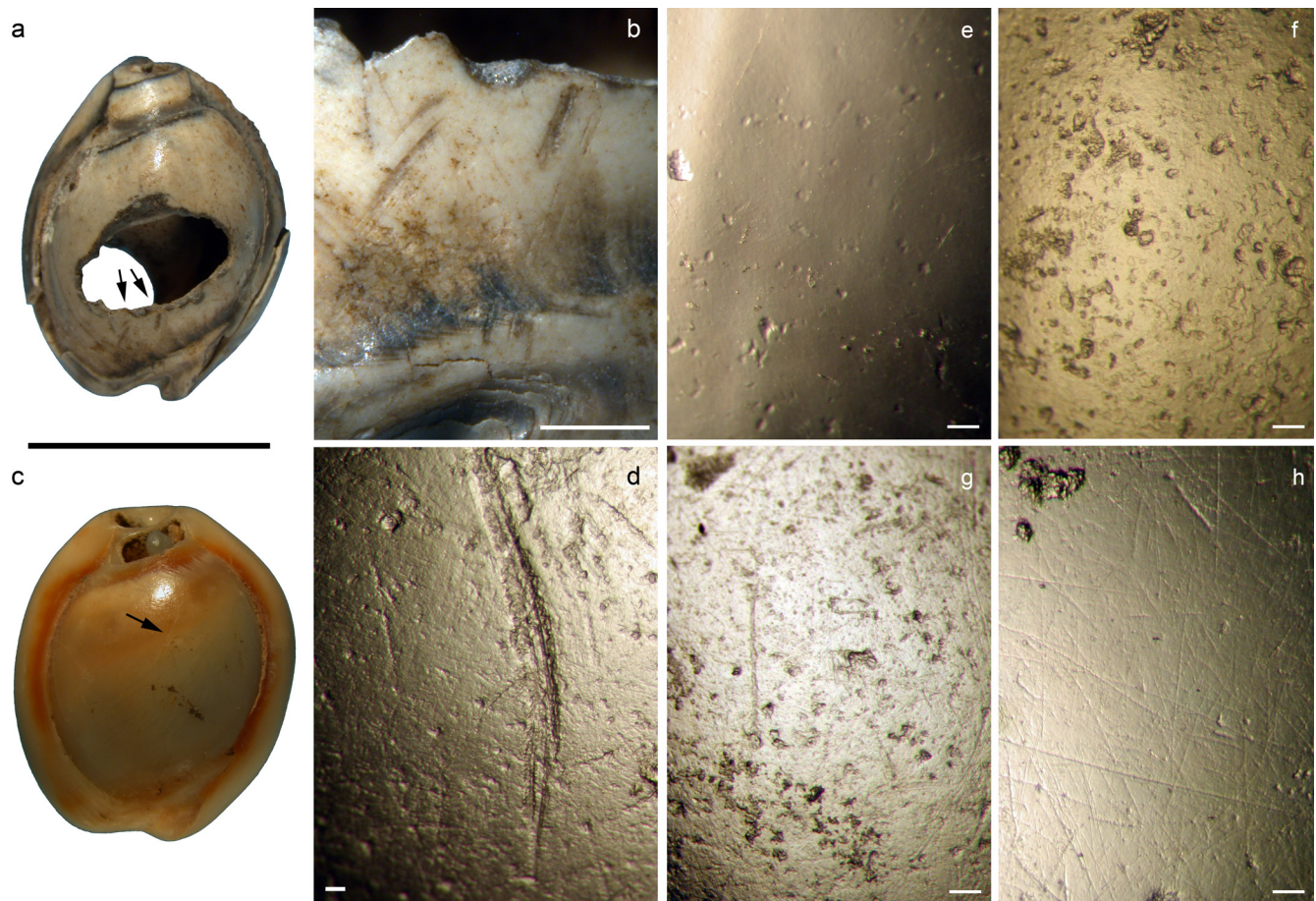


Fig. S4. (Left) Marks produced by stone tools on the dorsal side of two *Nassarius gibbosulus* from Grotte des Pigeons, Taforalt (a and b, n° TAF6871; c and d, n° 7025). (Right) Microscopic damage on the parietal shield of *Nassarius gibbosulus* shell from Djerba modern biocoenosis (e); Djerba modern thanatocoenosis (f); unperforated (g), and perforated (h) specimens from Taforalt (g, n° 7025; h, n° 7023). Notice the similarity between f and g and the wear pattern on h, characterized by a palimpsest of randomly oriented striations (Scale bars: a and c = 1 cm; b = 1 mm; d–h = 100 μ m.)

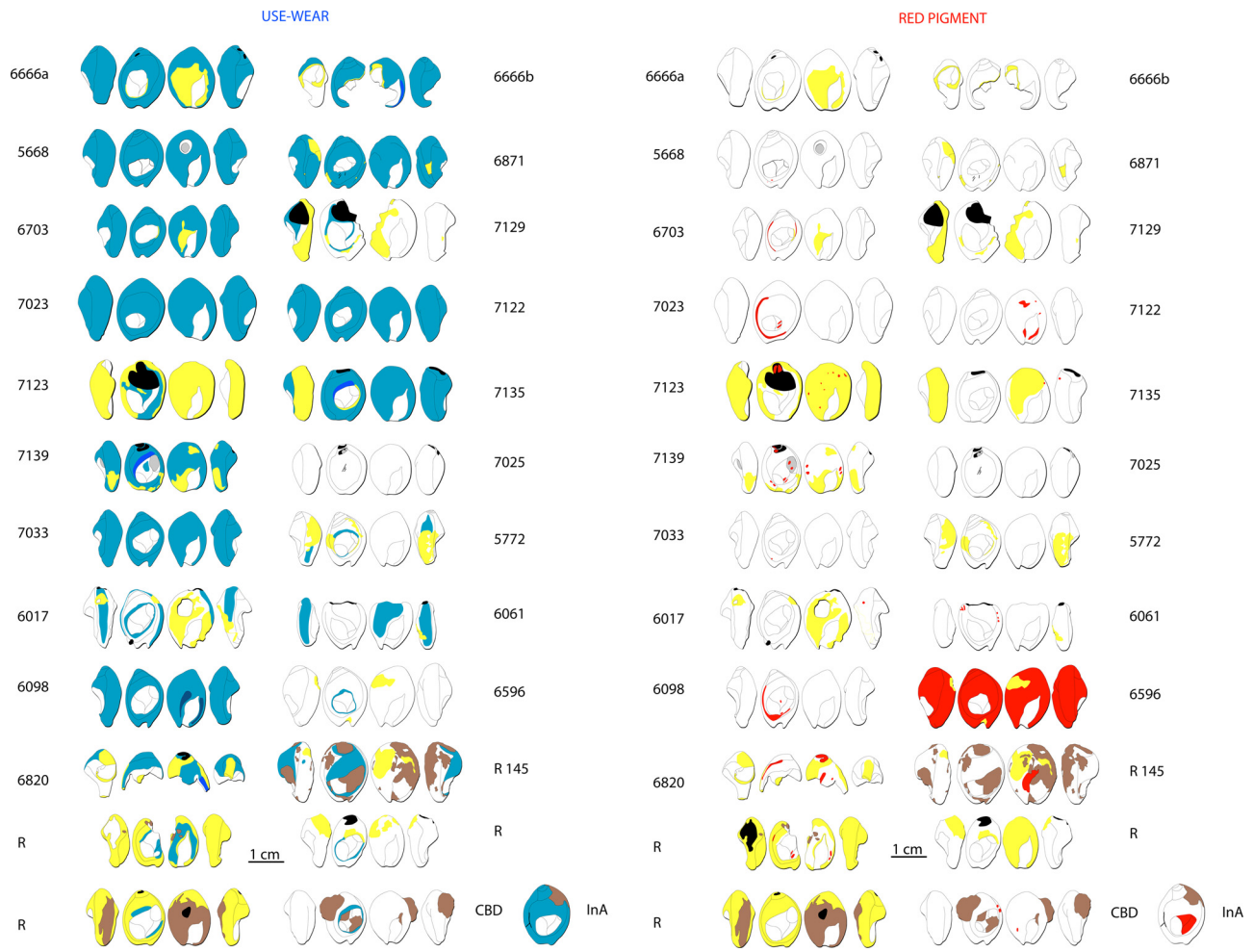


Fig. S5. Drawings of the *Nassarius* shells from Grotte des Pigeons (Taforalt), Rhafas (R), Contrebandiers (CBD), and Ifri n'Ammar (InA) indicating the location of the wear patterns (in blue) and pigment residues (in red). Wear facets are in dark blue. Altered areas and areas covered by concretions are in yellow and brown respectively.

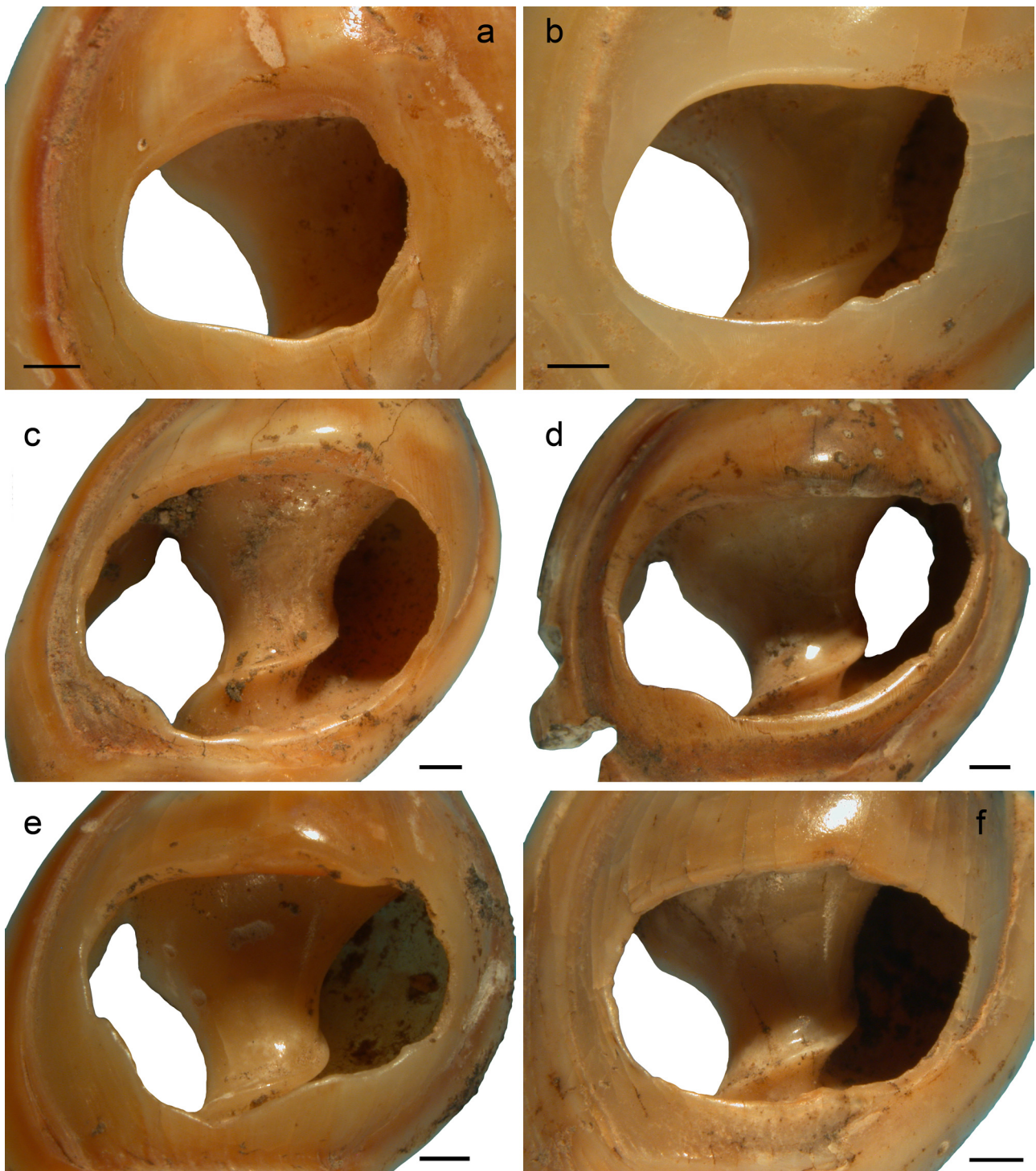


Fig. S6. Smoothed and heavily worn perforations on *Nassarius gibbosulus* shells from Grotte des Pigeons, Taforalt (a, n° 7023; b, n° 7122; c, n° 6098; d, n° 6017; e, n° 7033; f, n° 6703) (Scale bars: a–f = 1 mm.)

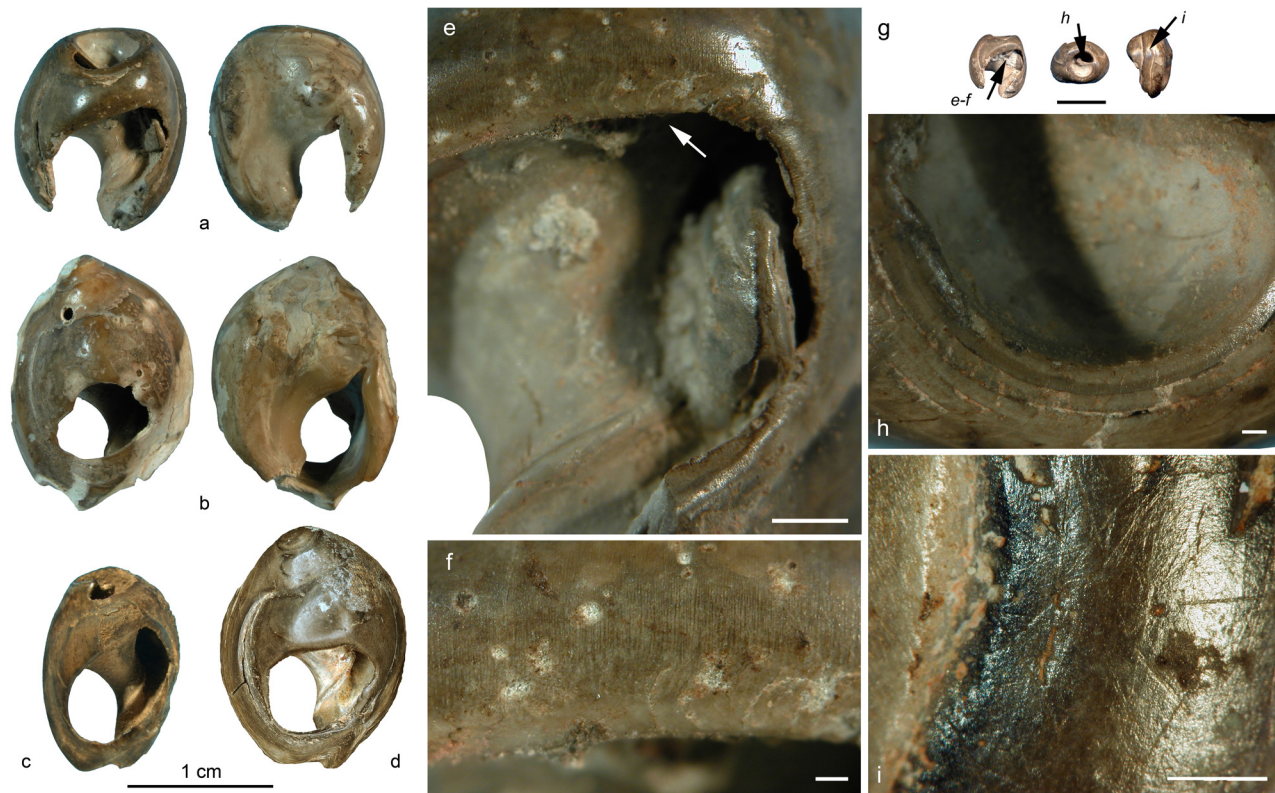


Fig. 57. *Nassarius gibbosulus* shells from Grotte des Pigeons, Taforalt (a and e–i, n° 3720; b, n° 5305), Rhafas (c), and Ifri n’Ammar (d) darkened by heating. Notice in a and e the presence of a fragment of bivalve stuck in the body whorl demonstrating that the burnt shell was collected when dead on the shore. Notice in e and f smoothed heat-cracks indicating the heated shell was subsequently affected by use-wear. Arrows in g indicate areas enlarged in e, f, h, and i; arrow in e indicates area enlarged in f. (Scale bars: e and f = 1 mm; g = 1 cm; h and i = 250 μ m.)



Fig. S8. *Nassarius gibbosulus* shells from Grotte des Pigeons, Taforalt, with residues of red pigment all over the surface (a–c, n° 6596) and in the groove between the parietal shield and the body whorl (d and e, n° 7023; f and g, n° 6098). Notice in b and c accumulations of pigment close to the siphonal canal and inside pits left by bioeroders. Arrow in a indicates the area enlarged in c, and arrow in d indicates the area enlarged in e. (Scale bars: a, d, and f = 1 cm; b, c, and g = 1 mm; e = 100 μ m.)

Table S1. Contextual and descriptive data on shells from the Middle Paleolithic layers of Grotte des Pigeons (Taforalt), Rhafas, Contrebardiers, and Ifri n'Ammar

Inv. n°	Sector	Square	Unit	Cult.	Chronol.	Species	Height, mm	Width, mm	PST 1, mm	PST 2, mm	Perf. (mm)		Perf. type**		Nat. alt.	He.	UseW.	O.	Fig. 1, n°
											dMax	dmin	dorsal	ventral					
Grotte des Pigeons																			
6666a	2	N14	E	Aterian	MIS 5e	<i>N. gibbosulus</i>	17,53*	13.42	4.26	5.64	7.99	6.15	f	a	-	●	a,b	-	1
6666b	2	N14	E	Aterian	MIS 5e	<i>N. gibbosulus</i>	14,07*	na	4.46	na	na	na	na	b	?	a,b,d	-	2	
157	2	L13	E	Aterian	MIS 5e	<i>N. gibbosulus</i>	16.92	11.99	5.99*	4.17*	5.77	5.98	f	c	a	●	na	-	***
5668	2	M14	E	Aterian	MIS 5e	<i>N. gibbosulus</i>	16.1	12.49	4.34	5.67	7.89	4.62	f	b	a,d	? a,b	●	3	
5348	2	M13	E	Aterian	MIS 5e	<i>N. gibbosulus</i>	13,06*	10.3	3,84*	3,64*	9.88	5.85	k	c	a,d,e	- a,b	●	***	
6871	2	N13	E	Aterian	MIS 5e	<i>N. gibbosulus</i>	14,98*	11.9	3.66	4.87	6.73	3.64	f	a	-	● a	-	4	
278	2	L13	E	Aterian	MIS 5e	<i>N. gibbosulus</i>	15,01*	11.13	3.94	5.48	5.81	4.22	g	a	-	- a,b	●	***	
1964	2	L15	E	Aterian	MIS 5e	<i>N. gibbosulus</i>	13,34*	10.73	4.57	4.32	na	na	c	a	d	-	●	***	
1965	2	L14	E	Aterian	MIS 5e	<i>N. gibbosulus</i>	14.47	10.72	4.27	4.58	6.73	5.06	f	a	-	- a,b,d,f	●	***	
2047	2	M17	E	Aterian	MIS 5e	<i>N. gibbosulus</i>	15.35	11.48	4.28	5.38	7.44	5.49	f	a	-	- a,b,d,e,f	●	***	
2087	2	M13	E	Aterian	MIS 5e	<i>N. gibbosulus</i>	12,74*	10.85	5.33	4.81	5.76	6.5	g	a	-	- a,b,d	●	***	
2022	2	M14	E	Aterian	MIS 5e	<i>N. gibbosulus</i>	14,97*	11.8	4.38	5.01	na	na	c	a	d	-	-	***	
5406	2	M14	E	Aterian	MIS 5e	<i>N. gibbosulus</i>	17.41	13.91	5.77	5.82	6.76	5.38	f	a	-	- a,b,e	●	***	
6703	1	L15	E	Aterian	MIS 5e	<i>N. circumcinctus?</i>	14,6*	10.61	4.76	4.05	6.78	4.43	f	a	-	?	a,b	●	5
7129	2	N14	E	Aterian	MIS 5e	<i>N. gibbosulus</i>	na	na	5.59	na	na	na	na	b	?	a,b,c	-	6	
7023	2	P12	E	Aterian	MIS 5e	<i>N. gibbosulus</i>	16,8*	13.29	4.25	5.76	5.94	4.3	f	a	-	- a,b,d,f	●	7	
7122	2	P13	E	Aterian	MIS 5e	<i>N. gibbosulus</i>	15.83	11.59	5.32	5.36	6.32	4.19	f	a	b	- a,b	●	8	
7123	2	P13	E	Aterian	MIS 5e	<i>N. gibbosulus</i>	na	12.72	na	na	na	na	a	-	?	c	●	9	
7135	2	P13	E	Aterian	MIS 5e	<i>N. gibbosulus</i>	na	12.36	4.19	5.01	7.37	5.21	g	a	-	- a,b,d,f	●	10	
7139	2	P13	E	Aterian	MIS 5e	<i>N. gibbosulus</i>	na	11.35	3.75	4.8	8.47	5.84	k	a	d,e	- a,b,c,f	●	11	
7025	2	M13	E	Aterian	MIS 5e	<i>N. gibbosulus</i>	13,97*	11.97	4.51	4.72	na	na	b	a	d	-	-	12	
7033	2	M14	E	Aterian	MIS 5e	<i>N. circumcinctus?</i>	15.44	10.93	3.43	4.96	8.03	4.52	j	a	-	- a,b,f	●	13	
5772	12	I14	E	Aterian	MIS 5e	<i>N. gibbosulus</i>	14.96	11.57	4.92	5.2	7.14	5.67	f	a	-	- a,b	-	14	
3367	2	N13	E+	Aterian	MIS 5e	<i>N. gibbosulus</i>	16.28	11.49	4.6	6.14	8.17	6.35	f	a	c	- a,b,f	-	***	
3368	2	N13	E+	Aterian	MIS 5e	<i>N. gibbosulus</i>	15.85	11.75	4.12	5.85	8.16	5.86	f	a	-	- a,b	●	***	
3720	2	P13	E+	Aterian	MIS 5e	<i>N. gibbosulus</i>	na	12.69	5.39	5.04	8.19	5.96	k	a	e	● a,b,f	●	***	
6017	2	P12	E++	Aterian	MIS 5e	<i>N. gibbosulus</i>	17.13	12,98*	na	4.94	9.85	5.64	j	c	a	- a,b	●	15	
6061	2	P12	E++	Aterian	MIS 5e	<i>N. gibbosulus</i>	na	12,17*	3.99	na	na	na	na	b	- a	●	16		
6098	2	P12	E++	Aterian	MIS 5e	<i>N. circumcinctus?</i>	16.53	11.11	4.04	4.83	9.13	6.34	j	a	-	- a,b,d,e	●	17	
6596	2	P12	E+	Aterian	MIS 5e	<i>N. gibbosulus</i>	17.06	12.77	4.5	5.05	6	4.98	f	a	b	- b	●	18	
6820	2	P12	E+	Aterian	MIS 5e	<i>N. gibbosulus</i>	na	na	na	na	na	na	na	na	-	- a,b,d	●	19	
5305	-	-	E+++	Aterian	MIS 5e	<i>N. gibbosulus</i>	na	13.3	5.15	5.96	6.8	5.57	f	d	-	● a	●	***	
Rhafas																			
145	-	D12	II-III	Aterian	MIS 5e/4	<i>N. gibbosulus</i>	16,69*	13.62	5.11	5,41*	11.19	5.78	k	a	b	- a,b	●	20	
-	-	-	-	-	-	<i>N. gibbosulus</i>	14,18*	na	3.58	na	na	na	na	-	- a,b,c	●	21		
-	-	-	-	-	-	<i>N. circumcinctus?</i>	14,76*	na	2.59	na	7.56	5.92	k	a	b	● a,b	-	22	
-	-	-	-	-	-	<i>N. gibbosulus</i>	15,94*	11.97	3.84	4.82	10.56	6.25	j	c	a	- b	-	23	
-	-	-	-	-	-	<i>Columbella rustica</i>	11*	10,5*	na	na	na	na	na	b	● a,b	●	24		
Contrebardiers																			
ES2	-	-	-	Aterian?	>MIS 3	<i>N. gibbosulus</i>	15.03	11.72	3.35	5.12	8.13	5.34	f	a	-	- na	●	25	
Ifri n'Ammar																			
-	-	-	MP-A	Aterian	MIS 5e	<i>N. gibbosulus</i>	17	12.3	-	-	-	f	-	-	● a,b	●	26		
-	-	-	MP-A	Aterian	MIS 5e	<i>Columbella rustica?</i>	15	10	-	-	-	na	na	-	- na	?	27		

Inv. n°, inventory number; Cult., cultural attribution; Chronol., chronology; MIS, marine isotope stage; +, burrow; ++, reworked; +++, sieving; PST 1, parietal shield thickness on the lip side; PST 2, parietal shield thickness on the side opposite to the lip; Perf., perforation; dMax, maximum diameter of the perforation; dmin, minimum diameter of the perforation; Nat. alt, natural alterations: a, perforation made by a gastropod predator; b, damage by bioeroders; c, encrustations; d, beach worn pebbles stuck inside; e, beach worn shells stuck inside; He, heating; UseW, use-wear; a, shine on prominent areas of the outer surface of the shell; b, smoothing of the perforation edge; c, smoothing on the spiral whorl; d, facet on the lip; e, facet on the parietal wall; f, facet on the edge of the perforation; O, ochre; *, affected by breakage; **, see Fig. 3; ***, shells already published in Bouzouggar et al. (1); na, not applicable.

1. Bouzouggar A, et al. (2007) 82,000-year-old shell beads from North Africa and implications for the origins of modern human behavior. *Proc Natl Acad Sci* 104:9964–9969.